A Grand Canonical Monte Carlo Study of the N 2 , CO, and Mixed N 2 –CO Clathrate Hydrates

Antoine Patt, Jean-Marc Simon, Sylvain Picaud, J. Marcos Salazar

A Grand Canonical Monte Carlo Study of the N_2, CO and Mixed N_2-CO Clathrate Hydrates

Antoine Patt,[†,‡] Jean-Marc Simon,[‡] Sylvain Picaud,[†] and J. Marcos Salazar[*,‡]

†*Institut UTINAM UMR 6213, CNRS/Université de Bourgogne Franche-Comté, Besançon, France*

‡*Laboratoire Interdisciplinaire Carnot de Bourgogne (ICB) UMR 6303, CNRS, Université de Bourgogne Franche-Comté, F-21078 Dijon Cedex, France*

E-mail: jmarcos@u-bourgogne.fr

Abstract

In this paper we report Grand Canonical Monte Carlo simulations to characterize the competitive trapping of CO and N_2 molecules into clathrates, for various gas compositions in the temperature range from 50 to 150 K. The simulations evidence a preferential trapping of CO with respect to N_2. This leads to the formation of clathrates that are preferentially filled with CO at equilibrium. This is irrespective of the composition of the gas phase, the fugacity and the temperature. Moreover, the results of the simulations show that the small cages of the clathrate structure are always filled in first place, and this is independent of either the guest structure or the temperature. This issue has been associated to the rather significant differences in the calculated heats of encapsulation ($\sim$2-3 kJ/mol) between the small and the larges cages. In addition, calculations with the simplified ideal adsorbed solution theory (IAST) are developed for allowing a comparison with the results arising from the GCMC simulations. Interestingly, this shows that the occupancy isotherms of the mixed N_2-CO clathrates can be perfectly represented by knowing the occupancy isotherms of the corresponding single-guest clathrates. This suggests that experiments performed with the single guest CO and N_2 clathrates might be sufficient to get information concerning the corresponding mixed clathrates by using the IAST approach.

Introduction

Gas hydrates are inclusion compounds made of H-bonded water molecules forming a network of small and large cages stabilized by encapsulated gaseous molecules.[1] These crystalline water-based solids, also known as clathrate hydrates, are thought to be ubiquitous on Earth, especially on the ocean floor and within the surface layer of the so-called permafrost (the frozen lands near the poles) where methane[1] is mainly trapped. The estimations of the amounts of gas stored in clathrates indicate that they are significantly greater than those from all the other sources of fossil fuels. Thus, clathrate hydrates are viewed as a potential energy resource for the future.[2] Clathrate hydrates are also at the heart of environmental concerns regarding the release of methane (which is a potent greenhouse gas) in the atmosphere. In this field of investigation, the possibility of exchanging CO_2 by CH_4 in a clathrate is of particular interest since it offers the possibility for reconciling energy production and greenhouse gas storage.[3]

Natural clathrate hydrates are also conjectured to be stable in various astrophysical environments (on other planets and/or their satellites, on comets and on Kuiper Belt objects).[4,5] Namely, their presence has been invoked either to explain the lack of noble gases in the atmosphere of Titan[6] or for understanding the composition of the interior lakes of Enceladus.[7]

The two most common clathrate structures found in natural environments are known as structures I (sI) and II (sII).[1] These structures differ by the arrangements of water cages present in the crystal lattice. That is to say, in sI clathrates small pentagonal dodecahedral cages, denoted 5^{12} (12 pentagonal faces in the cage) and large tetrakaidecahedral cages, denoted $5^{12}6^2$ (12 pentagonal faces and 2 hexagonal faces in the cage) are combined to form the water network. While in sII clathrates, the small 5^{12} cages are combined with large hexakaidecahedral cages, $5^{12}6^4$ (12 pentagonal faces and 4 hexagonal faces in the cage). Interestingly, the type of structure in which the water network will crystallize is largely subordinated to the size and shape of the encapsulated (or guest) molecule.

Among the clathrate hydrates of interest for extra-terrestrial environments, are the N_2

and CO hydrates. They are involved together with other gas hydrates like Xe-, Ar-, Kr-, H_2S-, NH_3-hydrates in the models of the formation of planetesimals and planetary atmospheres.[8] In these models, clathrate hydrates can be single-guest clathrates in which a single gas species is encapsulated within the cages or multiple-guest clathrate hydrates containing various species mixed together. The formation of multiple-guest clathrate hydrates has been suggested to be a probable sink for many chemicals occurring on Titan's surface.[9] Besides, the sequestration of several gases in CO_2- dominated clathrates may explain the different abundances of heavy noble gases in the atmospheres of terrestrial planets.[10] Recently, the formation of clathrate hydrates containing both N_2 and CO species has been considered for investigating, theoretically, the conditions of formation of the comet 67P/Churyumov-Gerasimenko.[11]

The composition of mixed clathrate hydrates at a given temperature and pressure can be estimated by means of the statistical mechanics approach developed by van der Waals and Platteeuw.[12] Their stability can be determined by using available codes such as the CSYMHD program that can give access to the dissociation curves.[1] However, the use of these approaches implies, from the theoretical point of view, a knowledge of the assumptions made and, in the case of simulations, the regions of validity of the parameterizations, generally obtained from experimental results (when available). Often this issue prevents the transferability of results to thermodynamical conditions other than those where the parameters were fitted.[1] These facts place numerical simulations based on an atomic-scale description of clathrates as a promising approach for characterizing the composition and the stability of clathrates, including multiple-guest ones. For this reason, molecular dynamics simulations have been frequently used for developing our understanding on these intriguing structures. For instance, recently the stability of a binary NH_3+THF (tetrahydrofuran) and CH_4+NH_3 clathrates from 100 to 240 K, in close relation with the corresponding experimental work has been studied.[13,14] In such simulations, usually performed on the canonical (N,V,T) or the isothermal–isobaric (N,p,T) ensembles, the number of molecules, N, in the simulated system

(here seen as the clathrate composition) is fixed. This last implies a strong dependence on the initial conditions. Here, we performed Grand Canonical Monte Carlo (GCMC) simulations[15] where the chemical potential is fixed rather than the number of the molecules. This allows to conveniently calculate the number of enclathrated molecules as a function of their imposed chemical potential. Notice that after the pioneering work of Tanaka *et al.*,[16,17] this method has been scarcely used for studying clathrate systems, even though it has proven its efficiency for calculating the composition of methane,[18–20] hydrogen,[21] ammonia[22] and binary hydrogen/THF[23] clathrates.

Recently, we have performed GCMC simulations for investigating the temperature dependence of the trapping inside a multiple-guest clathrate formed in contact with a gas mixture of CO and N_2, with proportions corresponding to the protosolar nebula (PSN).[11] These GCMC simulations were performed for temperatures ranging from 52 to 100 K, and completed via a thermodynamic extrapolation below 52 K. The aim of these calculations was to provide a physical interpretation of the measurements obtained for the comet 67P/Churyumov-Gerasimenko.[11] At very low temperatures and for CO/N_2 ratios typical of the PSN, CO was found to be preferentially incorporated in clathrate hydrates in comparaison to N_2, forming sI clathrates. Here, we extend this work by investigating extensively the selectivity in the N_2-CO mixed clathrate hydrates at higher temperatures and for different compositions of the gas phase in contact with the forming clathrate. We also characterize the selectivity for mixed clathrate of structure II because it has been recently evidenced that although CO and N_2 clathrate hydrates form initially in structure I (in a matter of days for N_2, of weeks for CO) they transform gradually to structure II.[24–26] Similarly, while mixed clathrates of N_2-CO remain stable in structure I when they are in contact with equimolar or CO dominated gas phases, a gas phase rich on N_2 may induce the sI-sII transformation of the mixed clathrate.[27]

The present paper is organized as follows. In Section 2 details of the GCMC simulations are given. The results concerning the occupancy isotherms for both single- and multiple-

guest clathrates systems and the selectivity of the mixed clathrates are discussed in detail in Section 3. Finally, in Section 4 the main conclusions of this study are summarized.

Simulations details

The trapping of CO and N_2 molecules in the clathrate hydrate lattice has been investigated by performing a set of Monte-Carlo (MC) simulations on the grand canonical (μ, V, T) ensemble at various temperatures ranging from 50 to 150K to characterize the influence of the temperature on the clathrate occupancy. Simulations have been performed by considering flexible clathrate, *i.e.*, a system where rotational and translational degrees of freedom of water molecules is allowed. In these simulations, while the number of water molecules in the simulation box has been kept constant, the number of CO and N_2 molecules hosted by the water network has been calculated by increasing the chemical potential, μ, of the gas phase in contact with the clathrate lattice.

These guest molecules were subjected to a grand canonical MC move. That is to say, not only translation and rotation but also insertion and deletion in the system is permitted. In addition, in the case of a mixed gas phase, swap of identity has been used for assuring the most energetically favorable configurations at high loading (in general at this loading the grand canonical move acceptance rate collapses). The swap move consists in substituting a molecule of a certain type by a molecule of another type, at the same position. The probabilities of the different MC moves have been set to 10% for translation, 10% for rotation, 40% for insertion/deletion and 40% for swap.

The isotherms, obtained as the average number of hosted molecules in the simulation box as a function of the chemical potential, will be referred below to as occupancy isotherms since we calculated the number of enclathrated molecules. The structures I and II considered are formed of $2 \times 2 \times 2$ unit cells taken from Takeuchi *et al.*[28] Periodic boundary conditions were applied to the simulation box, to mimic an infinite clathrate lattice. The simulated

system was then composed of 48 large and 16 small cages in the case of sI (containing 368 water molecules), and 64 large and 128 small cages for sII (1088 water molecules). The edge length of these cubic boxes was 24.06 Å and 34.62 Å in every direction, in agreement with the periodicity of the sI and sII clathrate lattices, respectively. Larger systems, up to $5 \times 5 \times 5$ cells, were also investigated for testing the fine size convergence on the calculated isotherms (which is one of the outcomes of the present study). Indeed, the obtained occupancy isotherms have shown an independence on the system size. Given this, only the results for the $2 \times 2 \times 2$ replica of the clathrate unit cells system are reported here.

As stated above, GCMC simulations relies on fixed chemical potential values to allow fluctuations in the number of particles in the system. This chemical potential can be expressed in terms of the fugacity which is convenient when handling gas mixtures. At low pressures, typically under 1 bar, one can assume that the fugacity of one species among a mixture corresponds to its partial pressure. A given mixture composition is then obtained by setting the fugacities with the right proportions. Beyond 1 bar, the non-ideality of the gas phase has to be taken into account, which can be easily done by using the fugacity coefficients associated with the species considered. Based on calculations fitted to experimental data,[29] N_2 fugacity coefficients remain close to 1, even at the highest temperatures and fugacities analyzed in our work. Considering that N_2 and CO are similar molecules, no significant deviation from ideality was expected for CO. This has been confirmed in the thermodynamic region of interest by obtaining similar densities from GCMC and from isothermal-isobaric (N,p,T) simulations for CO molecules only and with pressure being set equal to the fugacity used in the (μ, V, T) ensemble simulations.

In our MC simulations, performed using the GIBBS code,[30] 5×10^5 iteration steps were shown to be sufficient to ensure the equilibration of the systems considered. The equilibration phase has been followed by a production stage of 9.5×10^6 steps during which data have been collected for statistical analysis, giving a total of 10^7 MC simulation steps.

A classical description of the interaction potentials between water and guest molecules

has been used. Thus, the potential energy has been calculated as the sum of the pairwise Lennard-Jones (LJ) and Coulomb contributions of all pairs of various interaction sites located on the H_2O, CO and N_2 molecules. The water molecules have been represented using the TIP4P-Ew model[31] whereas the guest molecules have been modeled using the TraPPE force field for N_2[32] and the potential from the work of Piper *et al.,* for CO.[33] The Coulomb interactions have been computed with the Ewald summation technique whereas the LJ contributions to the interaction potential have been calculated using a cut-off equal to half the simulation box and by taking into account long-range corrections.[34] The interactions between two different LJ sites have been derived from the well-known Lorentz-Berthelot mixing rules (Table 1).

Different gas phase compositions have been investigated, ranging from 1:9 to 9:1 CO:N_2 ratios. However, given the global trends observed, we chose to report in the following only the results obtained at 50K, 100K and 150K and for the 1:3, 1:1 and 3:1 ratios. Moreover, before focusing on the mixed N_2-CO clathrate, the occupancy isotherms have been determined for both CO and N_2 sI and sII single-guest clathrates.

Results and discussion

CO and N_2 single guest Clathrates

The occupancy isotherms calculated for flexible single-guest clathrates, *i.e.*, the average number of either CO or N_2 molecules enclathrated as a function of the gas fugacity are given in Figure 1, for three temperatures: 50, 100 and 150 K. This figure gives the results for sI and sII clathrates in the top and the bottom rows, respectively. Remark that the fugacity axis is given on a logarithmic scale and that, on the y-axis, the number of enclathrated molecules has been divided by the total number of cages. Hence, given the simulation box size used here, an occupancy value of 1 corresponds to 64 and 192 guest molecules in sI and sII clathrate structures, respectively.

The comparison between the CO and the N_2 occupancy isotherms immediately shows that higher fugacities are always required to fill the clathrates with N_2 than with CO molecules. Overall, for any given fugacity and temperature, and for both sI and sII, the occupancy of the CO clathrate is higher than that of the N_2 one (Fig. 1). However, this difference of occupancy values decreases as the temperature increases. These results indicate that CO appears to be more easily enclathrated than N_2 irrespective of the temperature, and that sI and sII are filled at about the same fugacity values, irrespective of the guest species. It has also to be mentioned that the isotherms are, as expected, shifted toward higher fugacities when the temperature increases.

While most of the observed isotherms, for both CO and N_2, show a type I behavior (*cf.* IUPAC classification[35,36]), there is a noticeable difference at 50 K, between the occupancy isotherms simulated for the sI and sII clathrates. Indeed, in contrast with the sI isotherms which have a single-site Langmuir-like behavior, the shape of the occupancy isotherms for sII exhibits an inflection corresponding to an occupancy of ~ 0.65. This form of isotherm is characteristic of an adsorption process with two different energetic sites. This inflection is more accentuated for CO than for N_2, and is apparently missing for sI. Taking into account that the unit cell of a sII clathrate is made of 2/3 of small and 1/3 of large cages, the behavior of the corresponding occupancy isotherms strongly suggests that the occupancy of ~ 0.65 is associated to the loading of the small cages only, the large cages requiring thus higher fugacities to be occupied. By considering that CO and N_2 are small molecules with a respective diameter of 4.35 Å and 4.2 Å, we can infer that their interaction with water molecules tend to energetically stabilize first the small cages (7.82 Å in diameter) rather than the largest ones (9.46 Å in diameter). This could explain why this behavior is specially evidenced for the sII structure, because the large cages of sII are larger than those of the sI structure (with a diameter of 8.66 Å).

To check these assumptions we have also calculated the occupancy isotherms in small and large cages, separately. The results are given in Figures 2 and 3 for CO and N_2, respectively.

As it can be seen, at 50 K, the trapping of CO and N_2 molecules in the small cages occurs at lower fugacities than in the large cages, irrespective of the clathrate structure. Moreover, this preferential occupancy for the small cages is clearly more pronounced for CO than for N_2, and even more for structure II than for structure I. However, as expected from the analysis of the total adsorption isotherm (see Fig. 1), this preferential trapping in the small cages progressively disappears when increasing the temperature. This is in accordance with the results of the experiments which evidence the presence of CO (or N_2) molecules in both types of cages above 150 K (see Refs.[25–27]). In our simulations, at 150 K, both small and large cages exhibit similar occupancy in the case of CO. For N_2, the behavior is slightly different and a preferential trapping in the large cages is even visible. Moreover, the above mentioned features also agree with the behavior of calculated values of the Langmuir constants for small and large cages in structures I and II.[37] The calculated values at 50 K for small cages are higher than those for large cages which indicates that trapping in small cages would be preferred to any other configuration. At 150 K, the values of the Langmuir constants point to a similar trapping efficiency in both cage types for CO and a preferential trapping in the large cages for N_2. Note also that, at 100 and 150 K, occupancy values larger than one are also calculated at very high pressures, especially for CO in the large cages, indicating that multiple occupancy in some cages is also possible in these conditions.

To illustrate these findings at 50 K, we have characterized the positions of the CO molecules in the corresponding clathrates, by analyzing snapshots taken from the Monte Carlo simulations. As an illustration, Figure 4 shows the distribution, in the (x, y) plane, of the C and O atoms in a sII clathrate hydrate at 50 K. Each distribution was obtained by superimposing (along the (001) axis) 10^3 configurations taken from the simulation at a given fugacity. The results shown are for different fugacities and correspond to the first part of the isotherm ($f_a = 5 \times 10^{-10} Pa$), the inflection part of the isotherm ($f_b = 3 \times 10^{-9} Pa$) and the saturation of the clathrate ($f_c = 1 \times 10^{-5} Pa$). In Figure 4, while the C and O atoms are shown as black and red dots, respectively, the water molecules are not displayed for clarity.

Moreover, the geometrical centers of the small and large cages formed by the water network are indicated by blue and green circles, respectively. At low fugacity, Figure 4a shows that the large cages are almost empty while the small cages exhibit a much higher density of enclathrated molecules. At a fugacity value corresponding to the inflection part of the isotherm, we can observe on Figure 4b that even though every large cage is occupied at some point of the simulation, the small cages remain undoubtedly the main occupied cavities. Note that, because Figure 4 represents a projection along the (001) axis, a green circle corresponds to the superimposed occupancy of 2 larges cages, whereas a blue one represents the projection of 3 small cages. Nevertheless, the huge difference in the number of points represented in these circles clearly indicates that small cage occupancy has a much larger occurrence than large cage occupancy. By contrast, for high fugacity values, *i.e.*, when the saturation plateau of the isotherm is reached (Fig. 4c), the large cages are finally significantly occupied.

For understanding the different behaviors of CO and N_2, we have calculated the heat of encapsulation (adsorption heat) q for the clathrates studied here. In a GCMC simulation, it is straightforward to calculate q from both the fluctuations of the internal energy in the clathrate U^c and the fluctuations of the number N of molecules as[38]

$$q = RT - \frac{\langle \delta U^c \delta N \rangle}{\langle \delta N \delta N \rangle} \tag{1}$$

where $\langle \delta X \delta Y \rangle \equiv \langle XY \rangle - \langle X \rangle \langle Y \rangle$ and $\langle\rangle$ denotes an ensemble average in the grand canonical ensemble. R is the ideal gas constant and T the temperature.

The heats of encapsulation for the single-guest sI and sII clathrates considered here, at the temperature of 50 K, are given in Figure 5. In this figure, q is plotted as a function of the number of enclathrated molecules by unit cell. Notice that large fluctuations (indicated by errors bars) are obtained for q, coming from large energy fluctuations when considering flexible clathrates. Thus, the heats of encapsulation calculated for rigid clathrates are also given at the bottom of Figure 5 for comparison and exhibit much smaller error bars than for the flexible structures. Overall, these two figures clearly show that the heat of encapsulation

for CO is always lower than for N_2 ($\approx$ 10% lower), indicating that it is easier to trap CO than N_2, irrespective of the clathrate structure. Moreover, for the sI clathrate and for both CO and N_2, q is more or less constant independently of the clathrate loading up to a number of enclathrated molecules corresponding to the saturation. At saturation, very large fluctuations of q are obtained (even more pronounced for flexible than for rigid clathrates), corresponding to a dense phase where it is difficult to insert additional molecules. By contrast, for sII clathrates, q shows an abrupt increase of $\approx$ 2-3 kJ/mol for a loading of $\sim$ 16 molecules per unit cell which corresponds to the number of small cages in the unit cell of the sII clathrate. Above this loading (*i.e.*, when the large cages start to be occupied) the increase of q indicates that the large cages of sII are less energetic encapsulation sites, irrespective of the guest molecule. Moreover, the change in q for this loading is clearly larger for CO than for N_2. This is reflected in Figure 1 by the pronounced inflection in the CO occupancy isotherm and which is almost negligible for N_2 (at 50 K and for sII clathrates). Similarly, the heat of encapsulation for CO still remains lower than for N_2 at 100 and 150 K (Fig. 6), indicating that even at these temperatures CO seems more easily trapped than N_2 in the clathrates.

This preferential trapping for CO over N_2 in the hydrate could be related to differences in the interaction potential. Indeed, in contrast with the N_2-water electrostatic interactions which involves quadrupole-dipole interactions only, dipole-dipole contributions are also present in the case of the CO-water pairs. The importance of these dipole-dipole interactions has been recently evoked to explain the differences experimentally evidenced between CO_2-N_2 and CO_2-CO mixed gas hydrates.[39] Moreover, this feature fully agrees with the results of *ab initio* calculations which have shown that both CO-H_2O and N_2-H_2O interactions are dominated by electrostatic contributions, with differences coming from the additional dipole-dipole interactions in the case of the CO-H_2O dimers.[40] Finally, it is worth mentioning that the preferential trapping of CO with respect to N_2 has been experimentally recently observed during the PhD work of C. Petuya.[27]

Mixed CO-N_2 clathrate

The occupancy of clathrates formed in contact with a gas phase containing a mixture of CO and N_2 with different compositions has also been investigated by using GCMC simulations. The calculated partial occupancy isotherms (the isotherms giving separately the number of CO and the number of N_2 molecules enclathrated) are shown in Figures 7 and 8 for sI and sII, respectively. The top rows present the partial occupancy isotherms for three typical gas phase compositions, namely: 75% CO - 25% N_2 , 50% CO - 50% N_2, 25% CO - 75% N_2 at 50, 100 and 150 K. For any given gas phase composition, the partial occupancy isotherms clearly show that CO is preferentially encapsulated with respect to N_2. This last is valid for sI and sII mixed clathrates and, as in the case of single guest, irrespective of the fugacity and of the temperature. This result for mixed clathrates is in agreement with what could be inferred from simulations for the single-guest clathrates analyzed in the previous section. In a similar way, isotherms obtained for the mixed clathrates differ only at 50 K by a two-site adsorption process for the sII mixed clathrates (Fig. 8). In this case, the partial occupancy isotherms indicates that for fugacities lower than those corresponding to the inflection, there are practically no N_2 molecules in the mixed clathrate. Hence, we can assert that the structure is preferentially filled with CO molecules. The presence of concomitant and significant amounts of N_2 and CO molecules within the mixed clathrate, is observed only for larger values of the fugacity. This last is confirmed by the statistical analysis for the positions of C, O and N atoms with respect to the geometrical centers of small and large cages. Figure 9 shows that, at low fugacities, the mixed clathrate contains mainly CO molecules lodging preferentially in the small cages. Finally, increasing the fugacity above a certain threshold, also leads to the enclathration of N_2 molecules, with a marked tendency to occupy the large cages.

Besides the occupancy isotherms, we have also calculated the CO selectivity of the mixed clathrate, defined as $\frac{x_{CO}/y_{CO}}{x_{N_2}/y_{N_2}}$, where x_i and y_i are the mole fraction of species i in the clathrate hydrate and in the gas phase, respectively. The selectivities for the various mixed clathrates

considered here are given in the bottom rows of Figures 7 and 8 as a function of the fugacity and for three compositions of the gas phase. These figures show that the CO selectivity behaves similarly for the three compositions studied and it decreases as the temperature increases. Also, the CO selectivity remains more or less constant as the fugacity value is increased at 100 K and 150 K.

By contrast, at 50 K and for the sII clathrate, the CO selectivity is characterized by a sudden jump observed when the large cages start to be filled with N_2 and corresponding to the region where the inflection of the isotherm is observed. Our analysis also suggests that it may be the case for the sI clathrate, if we consider that the jump in the selectivity curves occurs for occupancy values close to 0.25. Indeed, this value corresponds to the percentage of small cages for sI. For all the cases analyzed, the CO selectivity is larger than 1 and indicates a preferential trapping of the CO with respect to the N_2 molecules. This is valid even for a gas phase containing 75 % of N_2. However, the selectivity for CO (*i.e.* the preferential trapping of CO in the mixed clathrate) decreases as the temperature increases.

The similarity of the occupancy isotherms for the single- and multiple-guest clathrates prompted us to develop an analysis based on the Ideal Adsorbed Solution Theory (IAST).[41] Briefly, IAST, which was developed by Myers and Prausnitz in 1965, allows to calculate multi-component adsorption isotherms using only its single component counterparts at the same temperature, by considering that the adsorbed species form an ideal mixture. This implies that both changes in enthalpy and in adsorbent area are negligible upon mixing of several species, and it gives rise to an expression analogous to Raoult's law for an adsorbed phase in equilibrium with a gas. Thus, if IAST satisfactorily reproduces the occupancy isotherms for the mixed clathrate, then this will suggest that the encapsulated CO-N_2 phase behaves as an ideal mixture. This approach has been previously used by Glavatskiy *et al.*,[3] to study the mixture CH_4-CO_2 in clathrates. They found at high pressures, that the mixture could not be considered as ideal due to the difference, especially in size, between CH_4 and CO_2 molecules.

We used the pyIAST Python package[42] for determining the IAST isotherms for the three CO-N_2 gas mixtures detailed above. As an illustration, these isotherms are compared to those obtained from GCMC simulations for an equimolar gas mixture of CO and N_2 in Figures 10 and 11 for structures I and II, respectively, at the three temperatures considered in the present study. As evidenced by these figures, isotherms obtained by using IAST and GCMC simulations are in excellent agreement. The isotherms for sI match remarkably well in the whole range of fugacities investigated irrespectively of the temperature (Fig. 10), indeed. Also when considering sII clathrates (Fig. 11), IAST and GCMC simulations we obtained practically identical results for a large range of fugacity values. Interestingly, the inflections observed at 50 K in GCMC simulations are also reproduced. We notice slight deviations between the IAST and GCMC results visible at the three temperatures considered at high fugacity values, only. The isotherms calculated with IAST indicate a higher fraction of CO molecules in the clathrate than with the GCMC isotherms. This may be related to the larger density of guest molecules in a saturated sII clathrate and thus to the fact that, in this situation, the (small) interactions between guests slightly influence their trapping at high fugacity. It is interesting to see in Figure 11, at 150 K, a large increase of the CO loading above 10^6 Pa. The combined amount of CO and N_2 molecules is larger than the number of available cages. This strongly suggests a double occupancy of some cages.

For assessing the validity of the IAST approach at different gas phase compositions, we compare the CO molar fractions in the clathrate (x_{CO}) calculated by IAST, as a function of the fraction of CO in the gas phase (y_{CO}), and those obtained by GCMC. An illustration of this comparison is depicted in Figure 12 for sI at 50 K. These calculations have been performed for several values of the fugacity, covering the whole isotherm range. As previously shown in Figure 10, both approaches give similar results for the CO molar fractions (irrespective of the gas phase composition). This advocates in favor of the IAST ideal model, if we exclude the small deviations for large y_{CO} and large fugacity values near saturation which are evidenced from GCMC results (Figures 10-11).

The accuracy of the IAST approach for the CO-N_2 clathrates can be understood in terms of weak interactions between the guest molecules. The energy distributions obtained by calculating the intermolecular interactions, E_{X-Y}, between two types of enclathrated molecules ($X, Y = CO, N_2$) show that N_2-N_2, N_2-CO and CO-CO interactions are comparable and less than 10 kJ/mol, as shown in Figures 13a and 13b for sI and sII, respectively. As a consequence of these rather weak interactions between CO and N_2, the enclathrated molecules act as an ideal mixture in the sense of IAST. In the light of these results, we can say that the CO-N_2 clathrate can be well described in the framework of the IAST simple model and this irrespectively of the temperature and gas phase composition. This suggest that, for this system, occupancy isotherms for single-guest clathrates are sufficient to characterize the corresponding multiple-guest clathrate.

Concluding remarks

In this paper, we have investigated the trapping of CO and N_2 molecules by sI and sII clathrates by performing Grand Canonical Monte Carlo simulations. These simulations include three different temperatures and various compositions of the gas phase. Here, the number of guest molecules incorporated into the water lattice, is calculated directly from GCMC simulations as a function of the fugacity. By considering single guest clathrates, our results revealed an enclathration process starting at lower fugacities for CO than for N_2 molecules. In addition, at any given fugacity, a clathrate can incorporate more CO than N_2 molecules. Interestingly, at low temperatures (*i.e.*, 50 K), the simulated occupancy isotherms evidenced a two-site adsorption behavior due to the fact that the small cages are more likely filled than the large cages. This result is related to differences in the calculated heats of encapsulation ($\sim$ 2-3 kJ/mol). In a similar way, our studies have shown that small cages were filled upstream and only after the large cages can be occupied.

As far as we know, there are no experimental measurements for the occupancy isotherms

for CO and N_2 clathrates in the range of temperatures considered in this work. Nonetheless, at least at 150 K, our results allow a qualitative comparison with a recent experimental works devoted to the stability of the CO and N_2 single-guest clathrates.[25,26] The experimental pressure range investigated would correspond in our studies to the saturation part of the occupancy isotherms (Fig. 1). In this case, our GCMC results indicate that both small and large cages are occupied. This issue is in agreement with the interpretation of the Raman spectra for both CO and N_2 clathrates. Moreover, the experimental results have evidenced that, whereas the small cages are always fully occupied, the large cages of sII clathrates can easily capture or release the guest molecules. This could also be related to the difference in the calculated heats of encapsulation for small and large cages.

Although the present GCMC simulations have considered flexible clathrate network, allowing thus possible changes of the cage geometries due to translation and rotation of the water molecules, it is worth mentioning that the calculations have been performed in the grand canonical ensemble. Thus, the volume of the simulation box has been kept constant during the simulations and expansion or contraction of the cages is not explicitly considered in the simulations. However, molecular dynamics simulations have been widely used to calculate the isothermal compressibility and the isobaric thermal expansion coefficients of clathrates with different water potential models. It has been shown that for, *e.*g., CH_4 and CO_2 hydrates, the size of the lattice constants does not vary more than 0.1 Å between 50 and 150 K at 1 bar, and this change is even less at 200 K in the [1-1000] bar pressure range.[43,44] Although similar studies are not available for CO and N_2 clathrates, we can also reasonably expect very little changes in the corresponding clathrate lattice structure upon CO and N_2 loading.

In addition to the single guest clathrates, a key point of our studies has been to characterize the occupancy in CO-N_2 mixed clathrates for various compositions of the gas phase. Our results undoubtedly evidenced a preferential trapping of CO with respect to N_2 and this is irrespective of the composition of the gas phase, the fugacity and the temperature. Such a

preferential CO trapping is consistent with the results at very low temperatures (below 100 K) for a gas phase composition typical of the protosolar nebula (87.1 % for CO and 12.9 % for N2).[11]

It is worth noting that GCMC is a powerful tool for investigating preferential guest trapping in multiple guest clathrates. It can, in principle, complement experimental investigations not only by giving a more detailed insight at the molecular level but also by exploring temperature and pressure ranges unreachable experimentally (*e.g.*, extra-terrestrial environnements). In addition, molecular simulations could also be used to compare the respective stability of the clathrate structures I and II by performing free energy calculations. However, experiments have shown that the clathrate structure can change with time, which is a strong indication that both kinetic and thermodynamic effects play an important role in the stabilization of the clathrates under consideration.[25,26,45] These structural transitions cannot be addressed by GCMC simulations since in this approach, the observables are obtained at equilibrium. In consequence, it might be cautious to consider that some of the systems investigated here can be in a metastable state.

Interestingly, the comparison between results arising from the simplified IAST model and from our simulations showed that the occupancy isotherms of the mixed CO-N_2 clathrates can be well reproduced by knowing only the isotherms of the corresponding single-guest clathrates. This excellent agreement can be associated to the comparable and rather weak interactions between guest molecules leading to a behavior as an ideal gas mixture. Finally, this last suggests that experiments performed on the single-guest CO and N_2 clathrates might be sufficient to get information on the corresponding mixed clathrates by using the IAST approach.

Acknowledgments

This project is supported by the French National Research Agency (ANR) in the framework of the MI2C project (ANR-15CE29-0016). Calculations have been performed thanks to the computational resources of the Centre de Calcul from the UBFC (Dijon-France).

References

(1) Sloan, E.; Koh, C. *Clathrate Hydrates of Natural Gases, Third Edition*; CRC Press: Boca Raton, USA, 2008.

(2) Kumar, S. Methane Clathratre: Dirty Fuel or Energy Savior: A New Form of Ice to Store Energy. *Int. Res. J. Eng. Tech.* **2015**, *02*, 1429–1438.

(3) Glavatskiy, K. S.; Vlugt, T. J. H.; Kjelstrup, S. Toward a Possibility to Exchange CO2 and CH4 in sI Clathrate Hydrates. *J. Phys. Chem. B* **2012**, *116*, 3745–3753.

(4) Mousis, O.; Lunine, J.; Picaud, S.; Cordier, D. Volatile Inventories in Clathrate Hydrates Formed in the Primordial Nebula. *Faraday Discuss.* **2010**, *147*, 509–525.

(5) Mousis, O.; Chassefière, E.; Holm, N.; Bouquet, A.; Waite, J.; Geppert, W.; Picaud, S.; Aikawa, Y.; Ali-Dib, M.; Rousselot, P. et al. Methane Clathrates in the Solar System. *Astrobiology* **2015**, *15*, 308–326.

(6) Mousis, O.; Lunine, J.; Picaud, S.; Cordier, D.; Waite, J.; Mandt, K. Removal of Titan's Atmospheric Noble Gases by their Sequestration in Surface Clathrates. *Astrophys. J. Lett.* **2011**, *740*, L9.

(7) Bouquet, A.; Mousis, O.; Waite, J.; Picaud, S. Possible Evidence for a Methane Source in Enceladus' Ocean. *Geophys. Res. Lett.* **2015**, *42*, 1334–1339.

(8) Mousis, O.; Lunine, J. I.; Thomas, C.; Pasek, M.; Marbœuf, U.; Alibert, Y.; Ballenegger, V.; Cordier, D.; Ellinger, Y.; Pauzat, F. et al. Clathration of Volatiles in the Solar Nebula and Implications for the Origin of Titan's Atmosphere. *Astrophys. J.* **2009**, *691*, 1780–1786.

(9) Osegovic, J.; Max, M. Compound Clathrate Hydrate on Titan's Surface. *J. Geophys. Res. Planets* **2005**, *110*, E08004.

(10) Mousis, O.; Lunine, J.; Petit, J.; Picaud, S.; Schmitt, B.; Marquer, D.; Horner, J.; Thomas, C. Impact Regimes and Post-Formation Sequestration Processes: Implications for the Origin of Heavy Noble Gases in Terrestrial Planets. *Astrophys. J.* **2010**, *714*, 1418–1423.

(11) Lectez, S.; Simon, J.-M.; Mousis, O.; Picaud, S.; Altwegg, K.; Rubin, M.; Salazar, J. M. A 32-70 K Formation Temperature Range for the Ice Grains Agglomerated By Comet 67 P/Churyumov-Gerasimenko. *Astrophys. J.* **2015**, *805*, L1.

(12) van der Waals, J. H.; Platteuw, J. . C. In *Advances in Chemical Physics*; Prigogine, I., Ed.; Wiley, 1959; Vol. II; Chapter Clathrate Solutions.

(13) Shin, K.; Kumar, R.; Udachin, K. A.; Alavi, S.; Ripmeester, J. A. Ammonia Clathrate Hydrates as New Solid Phases for Titan, Enceladus, and Other Planetary Systems . *Proc. Natl. Acad. Sci. U. S.A.* **2012**, *109*, 14785–14790.

(14) Alavi, S.; Shin, K.; Ripmeester, J. A. A Molecular Dynamics Simulations of Hydrogen Bonding in Clathrate Hydrates with Ammonia and Methanol Guest Molecules. *J. Chem. Eng. Data* **2015**, *60*, 389–397.

(15) Adams, D. J. Grand Canonical Ensemble Monte Carlo for a Lennard-Jones Fluid. *Mol. Phys.* **1975**, *29*, 307–311.

(16) Tanaka, H. The Thermodynamics Stability of Clathrate Hydrate. III. Accommodation of Nonspherical Propane and Ethane Molecules. *J. Chem. Phys.* **1994**, *101*, 10833.

(17) Tanaka, H. A Novel Approach to the Stability of Clathrate Hydrates: Grand Canonical Monte Carlo Simulation. *Fluid Phase Equilibr.* **1998**, *144*, 361–368.

(18) Sizov, V. V.; Piotrovskaya, E. M. Computer Simulation of Methane Hydrate Cage Occupancy. *J. Phys. Chem. B* **2007**, *111*, 2886–2890.

(19) Wierzchowski, S. J.; Monson, P. A. Calculation of Free Energies and Chemical Potentials for Gas Hydrates Using Monte Carlo Simulations. *J. Phys. Chem. B* **2007**, *111*, 7274–7282.

(20) Jin, D.; Coasne, B. Molecular Simulation of the Phase Diagram of Methane Hydrate: Free Energy Calculations, Direct Coexistence Method, and Hyperparallel Tempering. *Langmuir* **2017**, *33*, 11217–11230.

(21) Katsumasa, K.; Koga, K.; Tanaka, H. On the Thermodynamic Stability of Hydrogen Clathrate Hydrates. . *J. Phys. Chem. B* **2007**, *127*, 044509.

(22) Fàbiàn, B.; Picaud, S.; Jedlovsky, P.; Guilbert-Lepoutre, A.; Mousis, O. Ammonia Clathrate Hydrate As Seen from Grand Canonical Monte Carlo Simulations. *ACS Earth Space Chem.* **2018**, *2*, 521–531.

(23) Papadimitriou, N. I.; Tsimpanogiannis, I. N.; Papaioannou, A. T.; Stubos, A. K. Evaluation of the Hydrogen-Storage Capacity of Pure H_2 and Binary H_2-THF Hydrates with Monte Carlo Simulations. *J. Phys. Chem. C* **2008**, *112*, 10294–10302.

(24) Zhu, J.; Du, S.; Yu, X.; Zhang, J.; Xu, H.; Vogel, S. C.; Germann, T. C.; Francisco, J. S.; Izumi, F.; Momma, K. et al. Encapsulation Kinetics and Dynamics of Carbon Monoxide in Clathrate Hydrate. *Nat. Comm.* **2014**, *5*, 4128.

(25) Petuya, C.; Damay, F.; Talaga, D.; Desmedt, A. Guest Partitioning in Carbon Monoxide Hydrate by Raman Spectroscopy. *J. Phys. Chem. C* **2017**, *121*, 13798–13802.

(26) Petuya, C.; Damay, F.; Chazallon, B.; Bruneel, J. L.; Desmedt, A. Guest Partitioning and Metastability of the Nitrogen Gas Hydrate. *J. Phys. Chem. C* **2018**, *122*, 566–573.

(27) Pétuya-Poublan, C. Étude de la Stabilité, de l'Occupation des Cages et de la Sélectivité Moléculaire des Hydrates de Gaz par Spectroscopie Raman. Ph.D. thesis, Université de Bordeaux, 2017.

(28) Takeuchi, F.; Hiratsuka, M.; Ohmura, R.; Alavi, S.; Sum, A. K.; Yasuoka, K. Water Proton Configurations in Structures I, II, and H Clathrate Hydrate Unit Cells. *J. Chem. Phys.* **2013**, *138*.

(29) Holley, C., Jr.; Worlton, W.; Zeigler, R. *Compressibility Factors and Fugacity Coefficients Calculated from the Beattie-Bridgeman Equation of State for Hydrogen, Nitrogen, Oxygen, Carbon Dioxide, Ammonia, Methane, and Helium*; Los Alamos Scientific Lab., Los Alamos, NM (United States), 1958; Vol. 2271.

(30) Ungerer, P.; Tavitian, B.; Boutin, A. *Applications of Molecular Simulation in the Oil and Gas Industry : Monte Carlo Methods*; Editions Technip - IFP Publications: Paris, France, 2005.

(31) Horn, H. W.; Swope, W. C.; Pitera, J. W.; Madura, J. D.; Dick, T. J.; Hura, G. L.; Head-Gordon, T. Development of an Improved Four-Site Water Model for Biomolecular Simulations: TIP4P-Ew. *J. Chem. Phys.* **2004**, *120*, 9665–9678.

(32) Potoff, J. J.; Siepmann, J. I. Vapor Liquid Equilibria of Mixtures Containing Alkanes, Carbon Dioxide, and Nitrogen. *AIChE J.* **2001**, *47*, 1676–1682.

(33) Piper, J.; Morrison, J.; Peters, C. The Adsorption of Carbon Monoxide on Graphite. *Mol. Phys.* **1984**, *53*, 1463–1480.

(34) Allen, M.; Tildesley, D. *Computer Simulation of Liquids*; Oxford science publications: Oxford, 1987.

(35) IUPAC, Reporting Physisorption Data for Gas/Solid Systems wReference to the Determination of Surface Area and Porosity. *Pure Appl. Chem.* **1985**, *57*, 603–619.

(36) IUPAC, Recommendations for the Characterization of Porous Solids. *Pure Appl. Chem.* **1994**, *66*, 1739–1758.

(37) Lakhlifi, A.; Dahoo, P. R.; Picaud, S.; Mousis, O. A Simple Van't Hoff Law for Calculating Langmuir Constants in Clathrate Hydrates. *Chem. Phys.* **2015**, *448*, 53 – 60.

(38) Nicholson, D.; Parsonage, N. *Computer Simulation and the Statistical Mechanics of Adsorption*; Academic Press: Oxford, 1982.

(39) Petuya, C.; Damay, F.; Desplanche, S.; Talaga, D.; Desmedt, A. Selective Trapping of CO2 Gas and Cage Occupancy in CO2-N2 and CO2-CO Mixed Gas Hydrates. *Chem. Commun.* **2018**, *54*, 4290–4293.

(40) Sadlej, J.; Rowland, B.; Devlin, J. P.; Buch, V. Vibrational Spectra of Water Complexes with H2, N2, and CO. *J. Chem. Phys.* **1995**, *102*, 4804–4818.

(41) Myers, A. L.; Prausnitz, J. M. Thermodynamics of Mixed-Gas Adsorption. *AIChE J.* **1965**, *11*, 121–127.

(42) Simon, C. M.; Smit, B.; Haranczyk, M. PyIAST: Ideal Adsorbed Solution Theory (IAST) Python Package. *Comput. Phys. Comm.* **2016**, *200*, 364–380.

(43) Ning, F. L.; Glavatskiy, K.; Ji, Z.; Kjelstrup, S.; H. Vlugt, T. J. Compressibility, Thermal Expansion Coefficient and Heat Capacity of CH4 and CO2 Hydrate Mixtures Using Molecular Dynamics Simulations. *Phys. Chem. Chem. Phys.* **2015**, *17*, 2869–2883.

(44) Costandy, J.; Michalis, V. K.; Tsimpanogiannis, I. N.; Stubos, A. K.; Economou, I. G. Molecular Dynamics Simulations of Pure Methane and Carbon Dioxide Hydrates: Lattice Constants and Derivative Properties. *Mol. Phys.* **2016**, *114*, 2672–2687.

(45) Kuhs, W. F.; Chazallon, B.; Radaelli, P. G.; Pauer, F. Cage Occupancy and Compressibility of Deutered N_2-Clathrate Hydrate by Neutron Diffraction. *J. Inclusion Phenom. Mol. Recognit. Chem.* **1997**, *29*, 65–77.

Figures and tables

Table 1: Parameters of the interaction potentials used in the GCMC simulations, for the water,[31] CO[33] and N_2[32] molecules. Distances and σ are given in Å, ε in K and charges in atomic units. Note that M, Q_{ext1} and Q_{ext2} represent the additional sites in the TIP4P-Ew model of water[31] and in the interaction potential model for CO,[33] respectively.

water	r_{OH}	r_{OM}	∠ HOH	σ	ε	q
	0.9572	0.1250	104.52°			
O				3.16435	81.90	0.0
H				0.0	0.0	0.52422
M				0.0	0.0	−1.04844
CO	r_{CO}	$r_{CQ_{ext1}}$	$r_{OQ_{ext2}}$	σ	ε	q
	1.1282	0.4374	0.158			
C				3.385	39.89	0.831
O				2.885	61.57	0.0
Q_{ext1}				0.0	0.0	−0.636
Q_{ext2}				0.0	0.0	−0.195
N_2	r_{NN}		∠ NN	σ	ε	q
	1.10		180°			
N				3.31	36.0	−0.482
center of mass				0.0	0.0	0.964

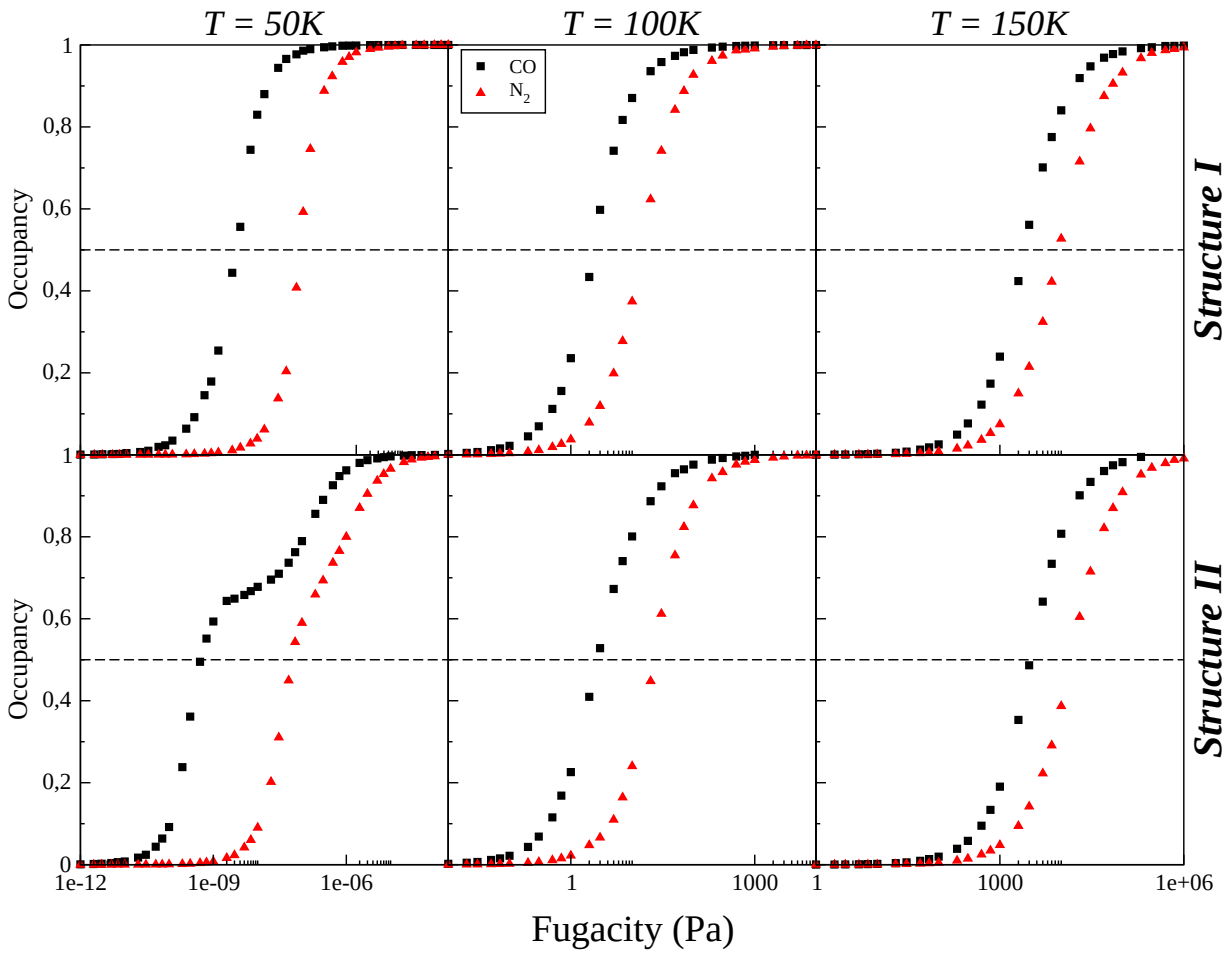

Figure 1: Occupancy isotherms of CO (black squares) and N_2 (red triangles) single-guest sI (top) and sII (bottom) clathrate hydrates as a function of the fugacity, at T=50K, 100K and 150K, as computed by GCMC simulations. The error bars are smaller than the symbols.

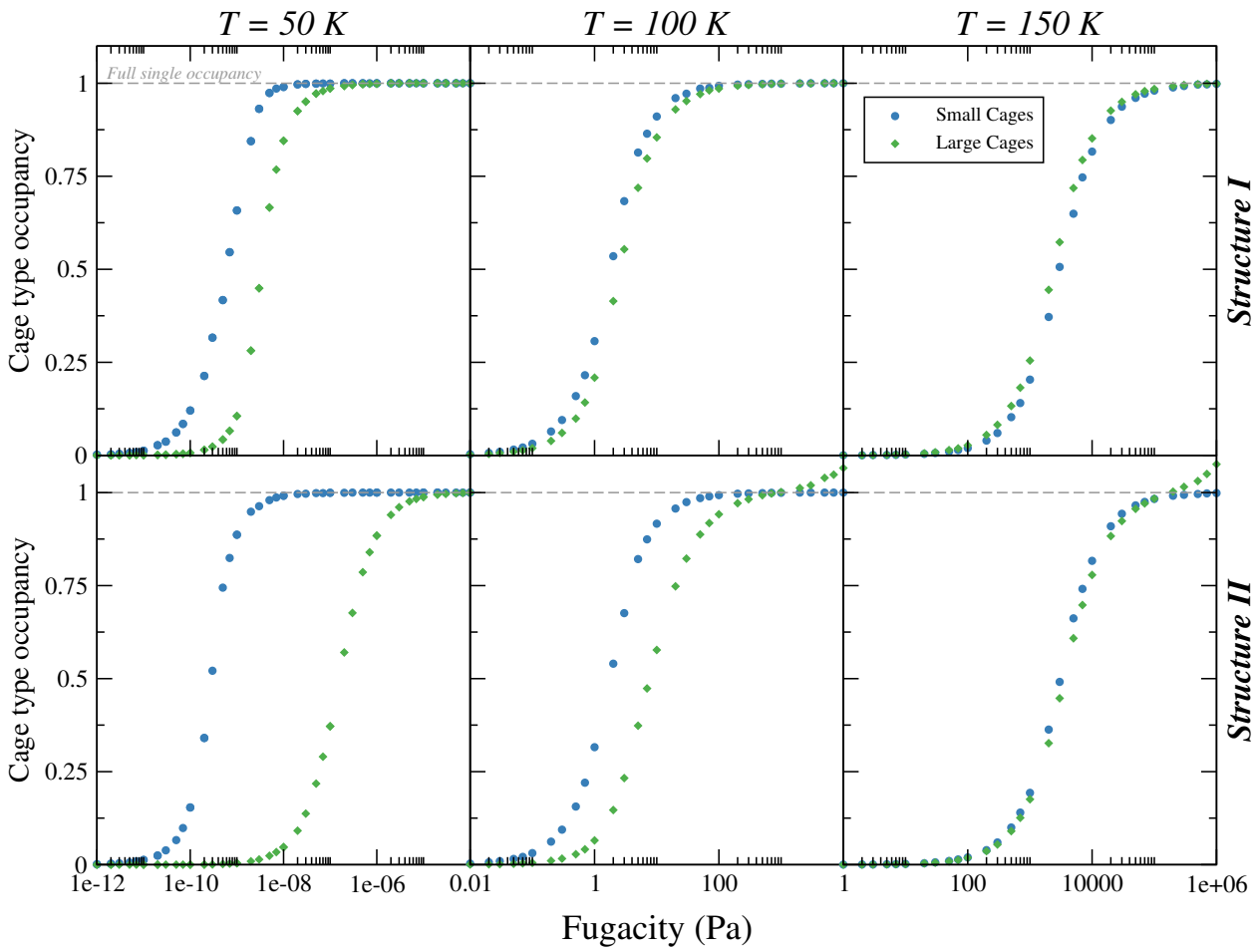

Figure 2: Occupancy isotherms for the small cages (blue circles) and large cages (green diamond) calculated separately, in the case of the CO single-guest sI (top) and sII (bottom) clathrate hydrates as a function of the fugacity at T=50K, 100K and 150K, as computed by GCMC simulations.

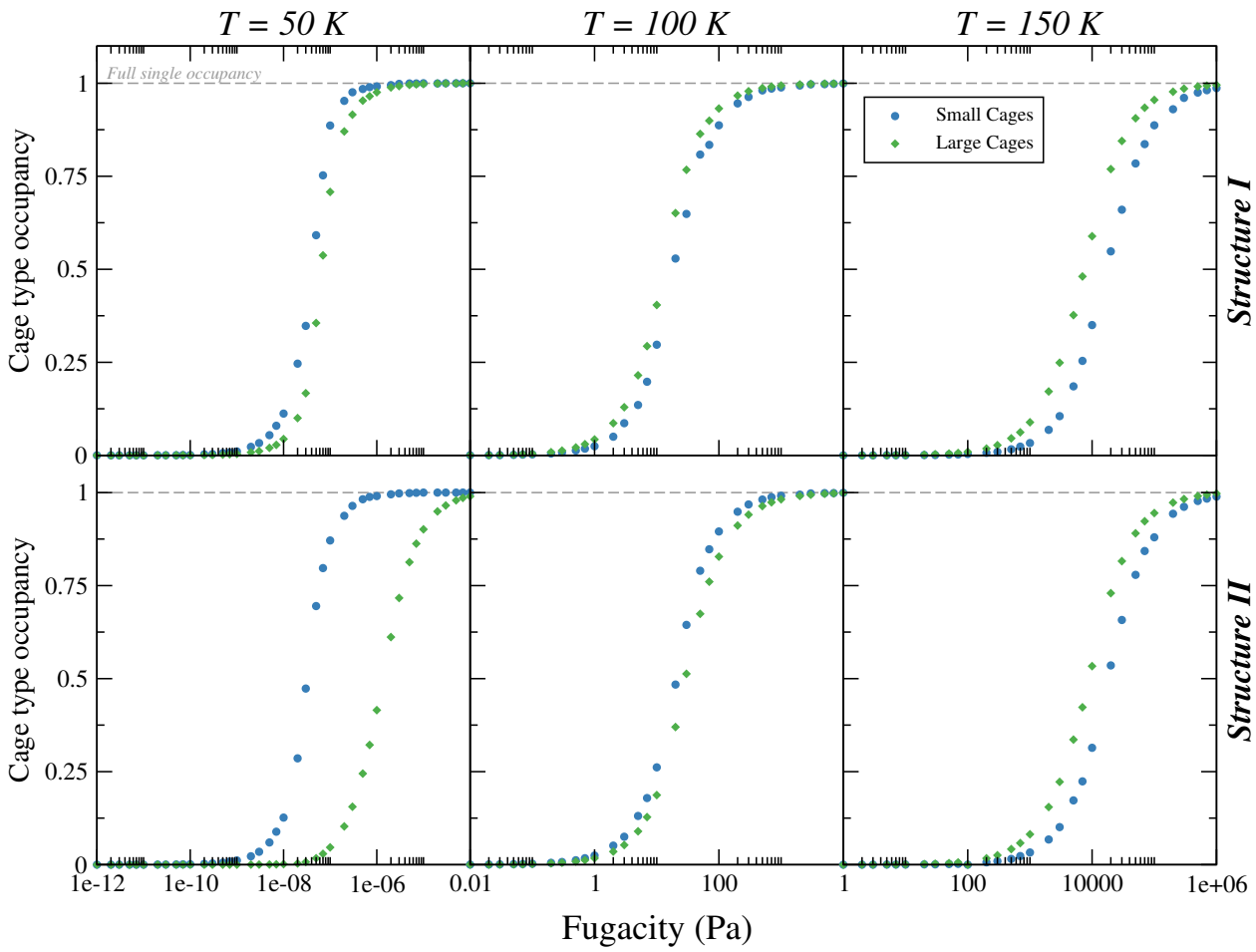

Figure 3: Occupancy isotherms for the small cages (blue circles) and large cages (green diamond) calculated separately, in the case of the N_2 single-guest sI (top) and sII (bottom) clathrate hydrates as a function of the fugacity at T=50K, 100K and 150K, as computed by GCMC simulations.

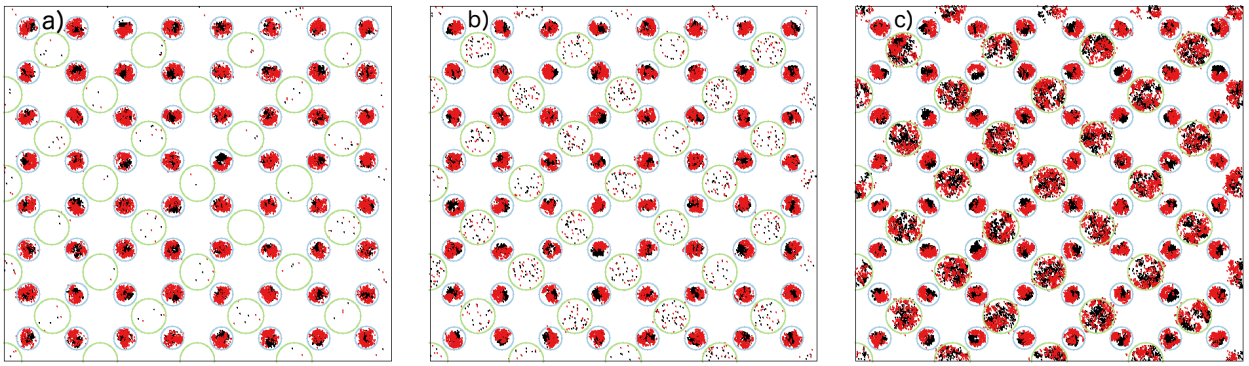

Figure 4: Spatial distributions in the (x, y) plane of CO molecules encaged in a $2 \times 2 \times 2$ structure II clathrate, for three different fugacities corresponding to (a) the beginning of the isotherm ($f_a = 5 \times 10^{-10} Pa$), (b) the inflection part ($f_b = 3 \times 10^{-9} Pa$) and (c) the saturation of the hydrate ($f_c = 1 \times 10^{-5} Pa$). These distributions correspond to the superimposition, along the (001) axis, of 10^3 configurations taken from the simulations. Carbon and oxygen atoms are represented by black and red dots, respectively. The water molecules are not shown for clarity. The geometrical centers of the small and large cages formed by the water network are indicated by blue and green circles, respectively.

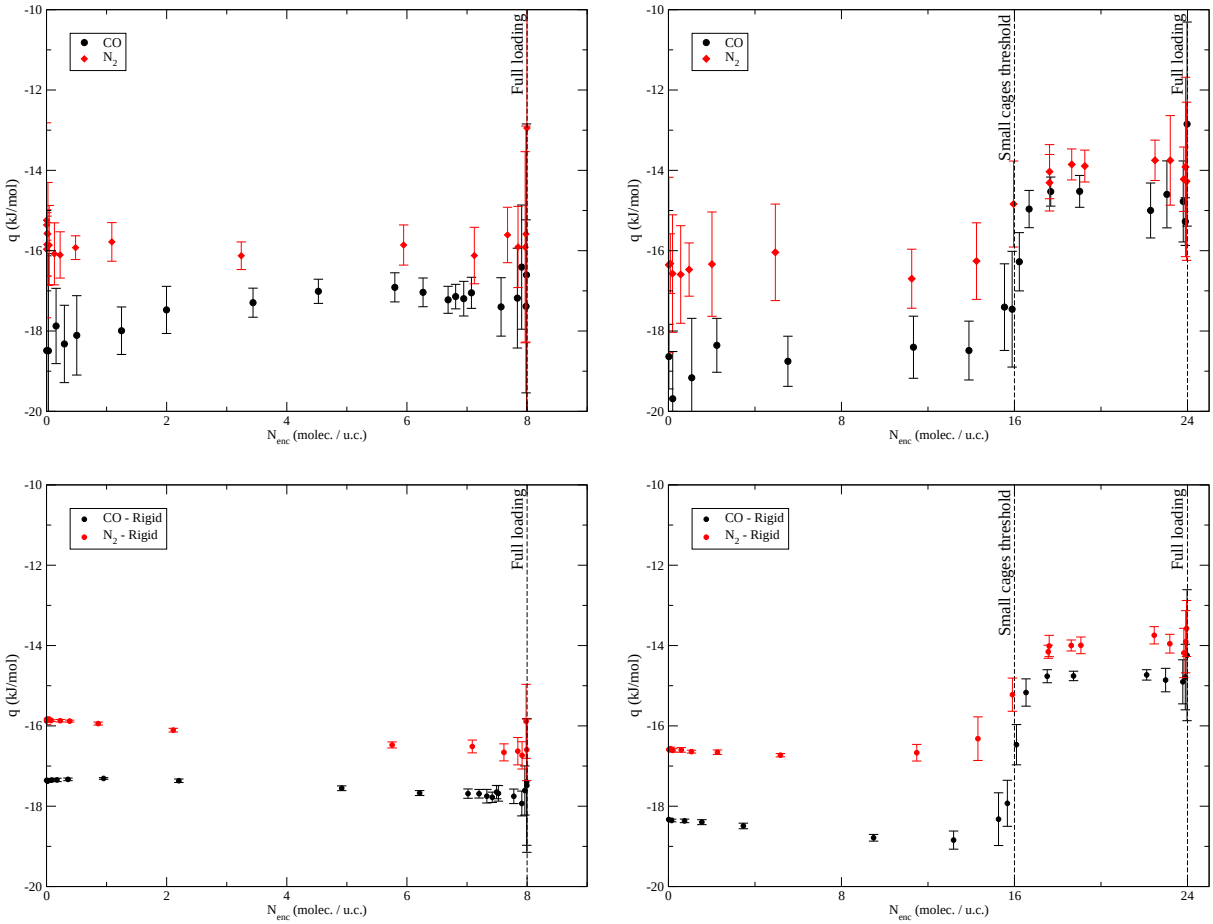

Figure 5: Heat of encapsulation for sI (left) and sII (right), flexible (top) and rigid (bottom) clathrates as a function of the number of enclathrated molecules per unit cell, at T=50K. Results for the CO and N_2 clathrates are represented in black and red, respectively.

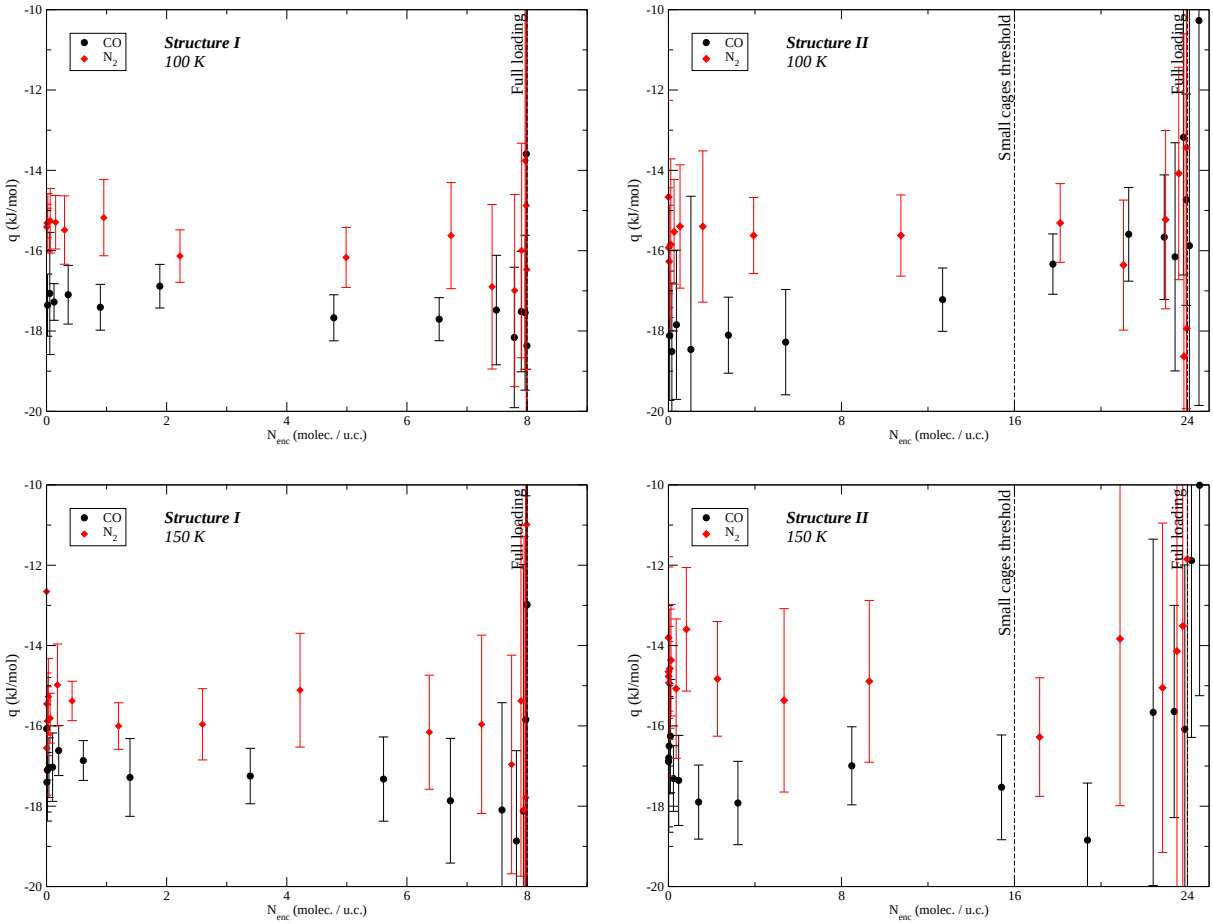

Figure 6: Heat of encapsulation for sI (left) and sII (right) flexible clathrates as a function of the number of enclathrated molecules per unit cell, at T= 100 K (top) and 150 K (bottom). Results for the CO and N_2 clathrates are represented in black and red, respectively.

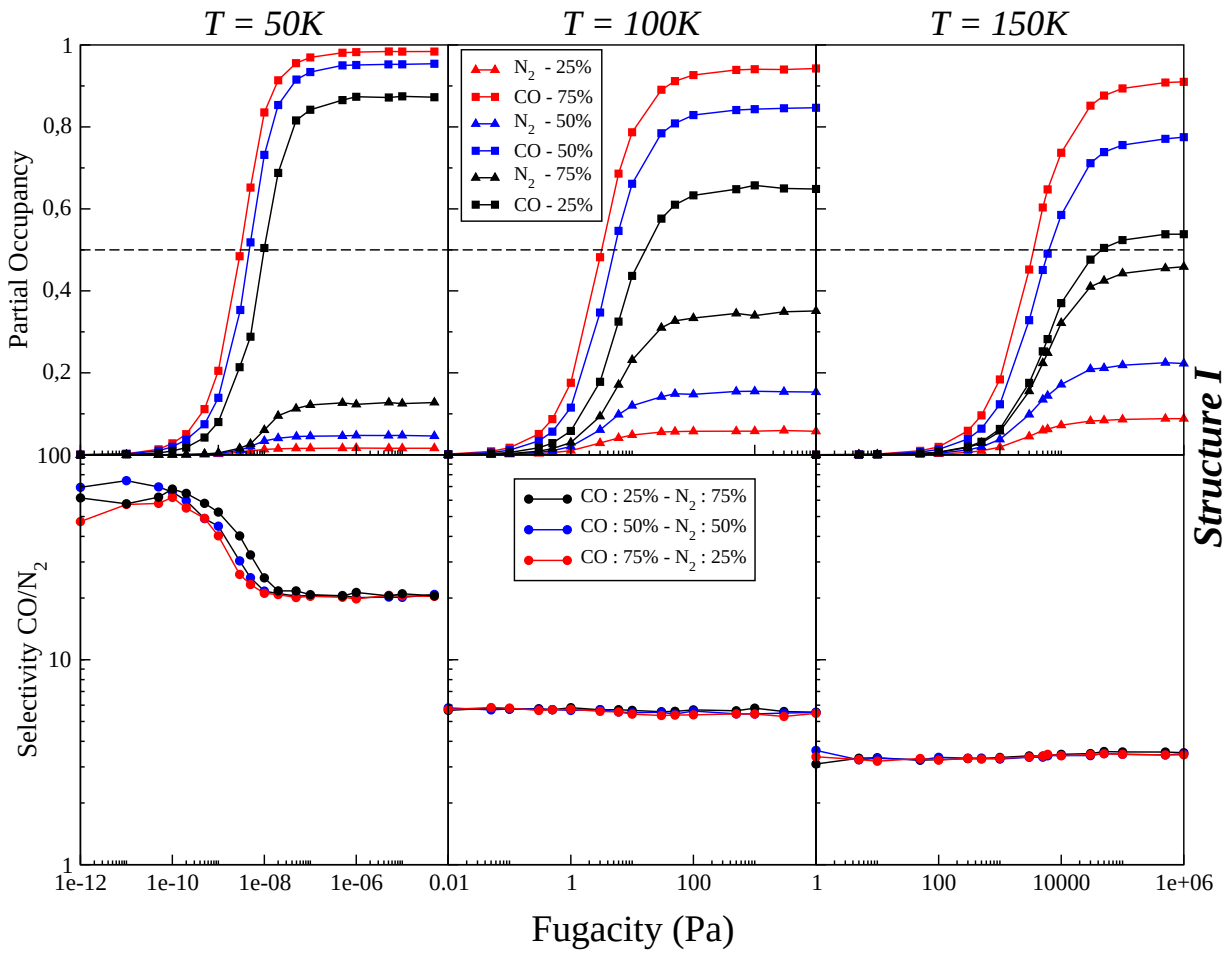

Figure 7: Partial occupancy isotherms (top), and the corresponding CO selectivities (bottom), of mixed CO-N_2 clathrate hydrates as a function of the fugacity, for structure I, at 50, 100 and 150 K. Lines are guide for the eye, only.

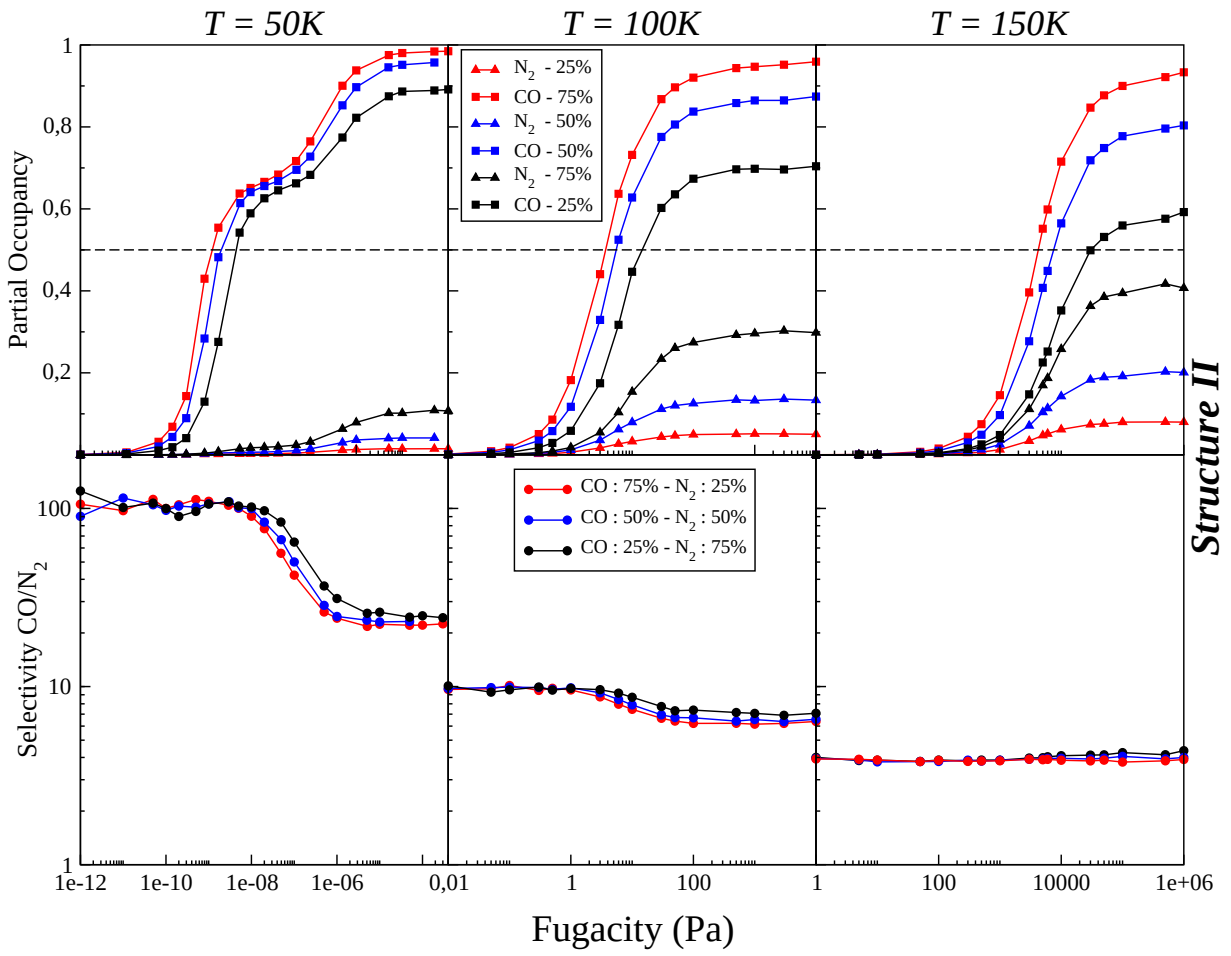

Figure 8: Partial occupancy isotherms (top), and the corresponding CO selectivities (bottom), of mixed CO-N_2 clathrate hydrates as a function of the fugacity, for structure II, at 50, 100 and 150 K. Lines are guide for the eye, only.

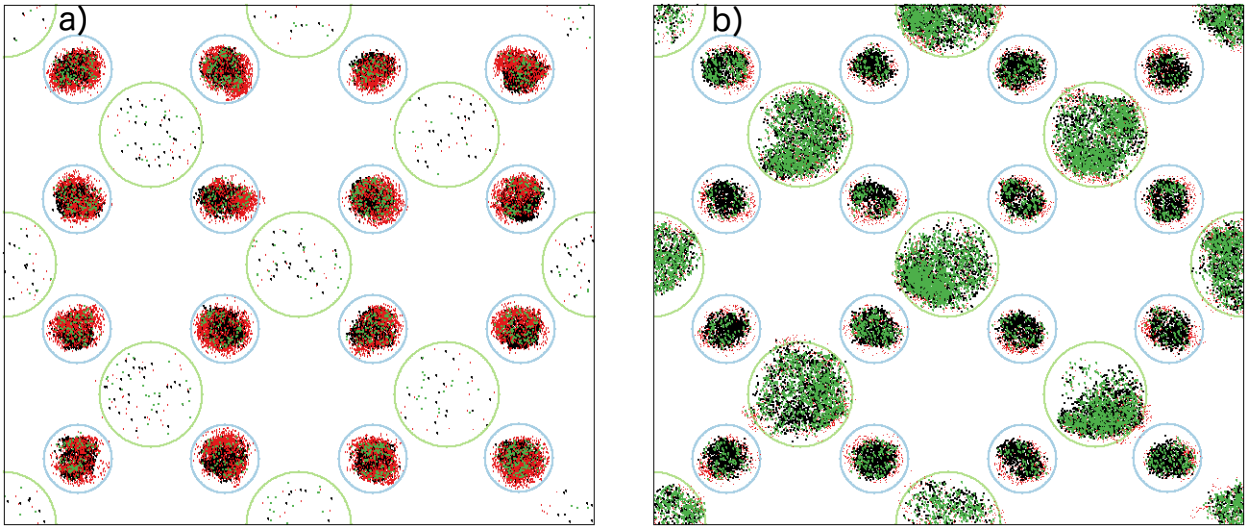

Figure 9: Spatial distributions in the (x, y) plane of CO and N_2 molecules encaged in a $2 \times 2 \times 2$ structure II clathrate, for two different fugacities corresponding to (a) the inflection part ($f_a = 1 \times 10^{-8} Pa$) and (b) the saturation of the hydrate ($f_b = 1 \times 10^{-4} Pa$). These distributions correspond to the superimposition of 10^3 configurations taken from the simulations. Carbon, oxygen and nitrogen atoms are represented by black, red, and green dots, respectively. The water molecules are not shown for clarity. The geometrical centers of the small and large cages formed by the water network are indicated by blue and green circles, respectively. Only a part of the hydrate is shown in this figure. For clarity, it is important to indicate that the black dots are first plotted then the red and the green. This can give a misleading impression that nitrogen is more abundant than CO in (b).

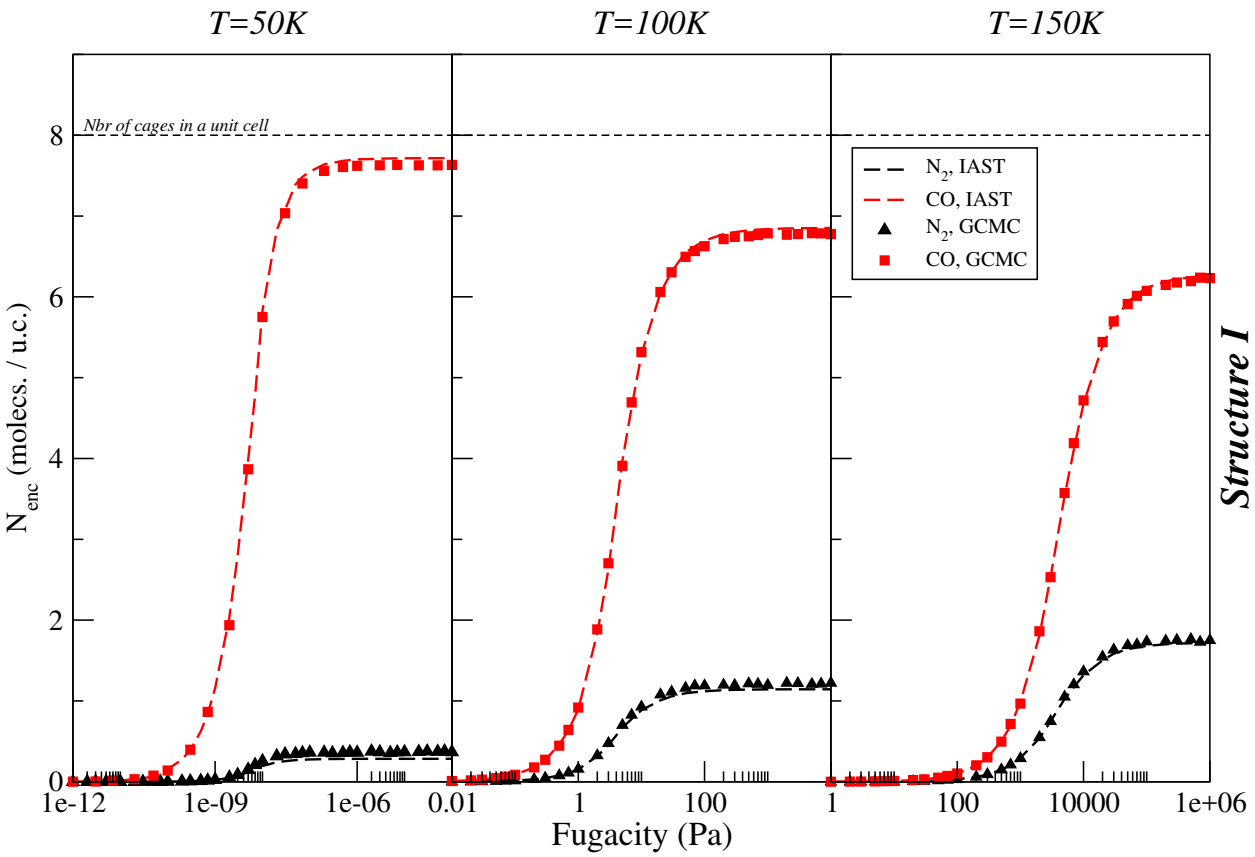

Figure 10: Comparison between isotherms (in black and red colors for CO and N_2, respectively) calculated by using the IAST approach (dashed curves) and those obtained from GCMC simulations (symbols), for structure I at 50, 100 and 150K, and for an equimolar mixture of CO and N_2.

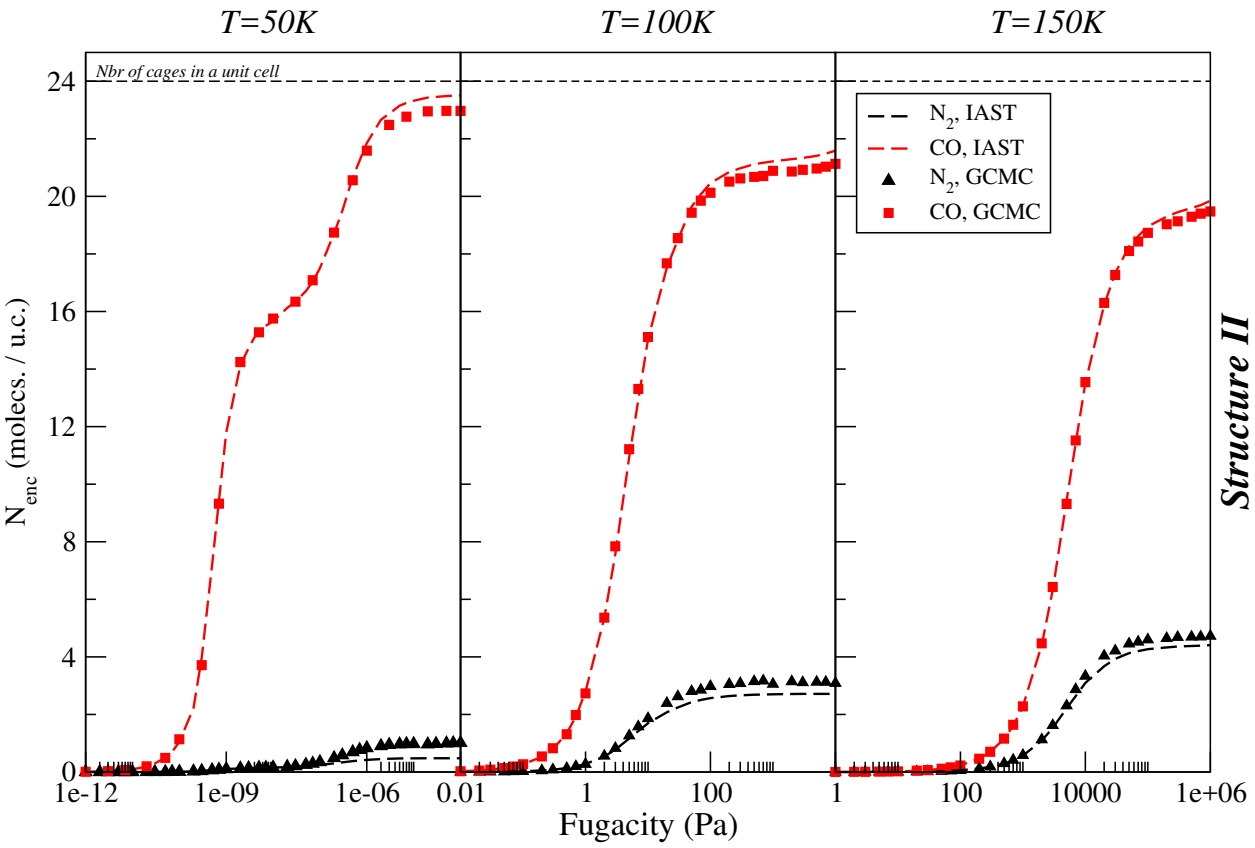

Figure 11: Comparison between isotherms (in black and red colors for CO and N_2, respectively) calculated by using the IAST approach (dashed curves) and those obtained from GCMC simulations (symbols), for structure II at 50, 100 and 150K, and for an equimolar mixture of CO and N_2.

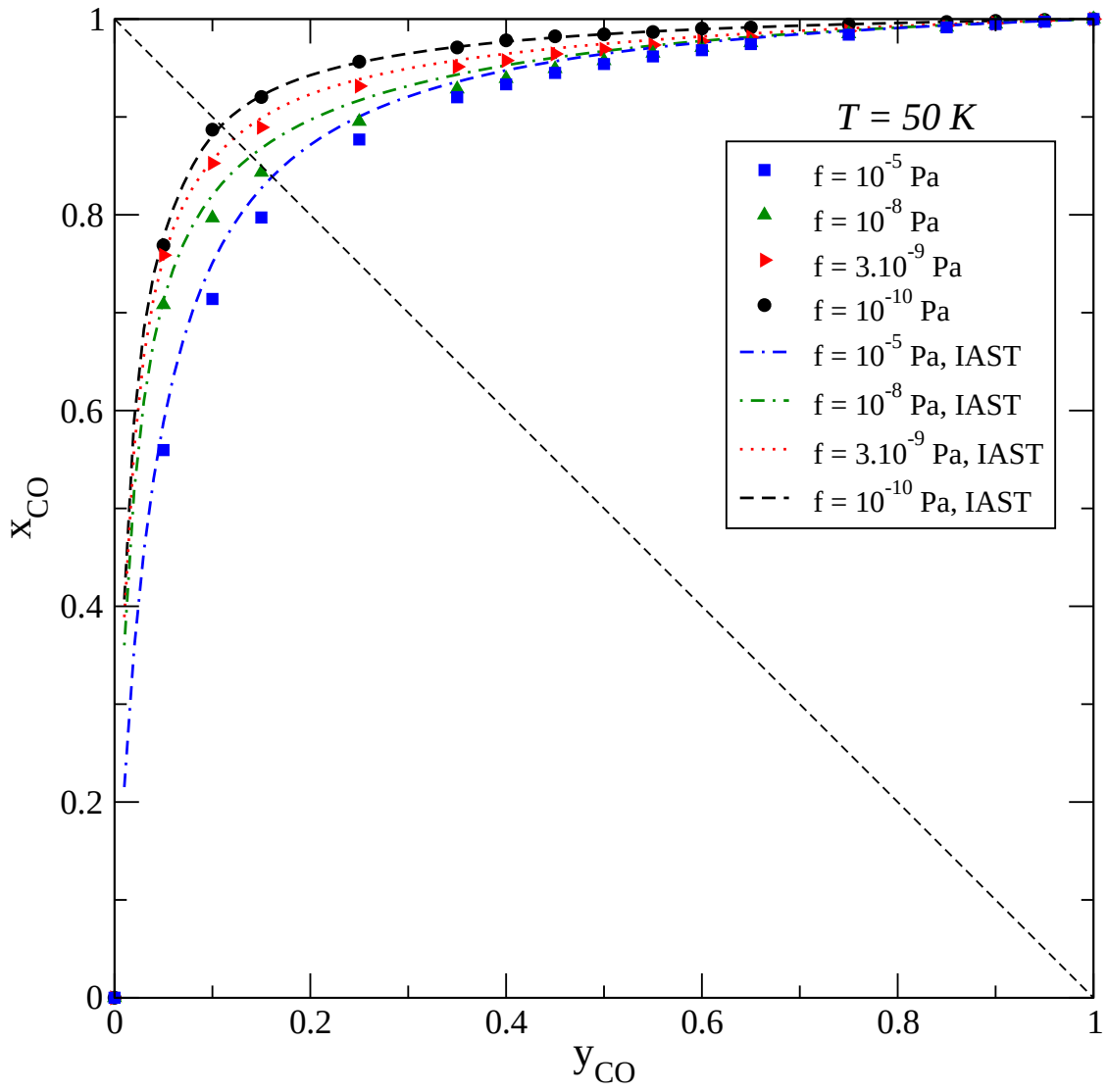

Figure 12: Comparison between the IAST (dashed curves) and GCMC (symbols) calculations for the CO molar fraction in the sI clathrate hydrate as a function of the CO molar fraction in the gas phase. The comparisons are done for fugacities of 10^{-10} (black dots), 3×10^{-9} (red triangles), 10^{-8} (green triangles) and 10^{-5} (blue squares) Pa, at a temperature of 50 K.

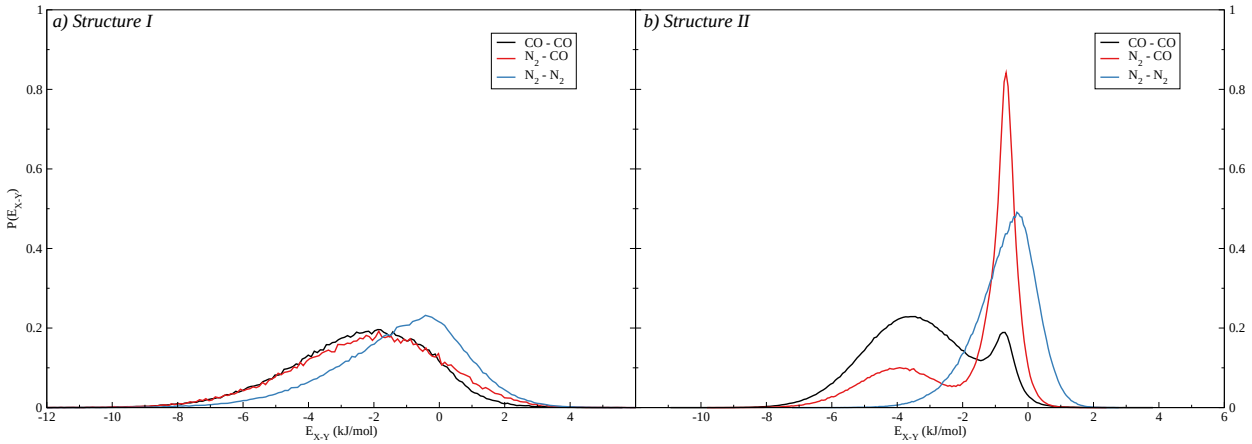

Figure 13: Distribution of the interaction energies (in kJ/mol), E_{X-Y}, between guest molecules (X, Y = CO,N_2) encapsulated within a sI (a) left panel) and a sII (b) right panel) clathrates at 50 K and at saturation. This was obtained for clathrates in contact with a gas phase of a N_2:CO ratio of 90:10 in order to a sufficiently large numbers of enclathrated N_2 molecules.

Graphical TOC Entry